

**Nuclear fusion reactions in deuterated metals**

Vladimir Pines,<sup>1,\*</sup> Marianna Pines,<sup>1</sup> Arnon Chait<sup>2</sup>, Bruce M. Steinetz<sup>2</sup>, Lawrence P. Forsley<sup>3</sup>, Robert C. Hendricks,<sup>2</sup> Gustave C. Fralick,<sup>2</sup> Theresa L. Benyo<sup>2</sup>, Bayarbadrakh Baramsai<sup>4</sup>, Philip B. Ugorowski<sup>4</sup>, Michael D. Becks,<sup>4</sup> Richard E. Martin<sup>5</sup>, Nicholas Penney<sup>6</sup>, and Carl E. Sandifer, II<sup>2</sup>

<sup>1</sup>*PineSci Consulting, Avon Lake, Ohio 44012, USA*


<sup>2</sup>*National Aeronautics and Space Administration, Glenn Research Center, Cleveland, Ohio 44135, USA*

<sup>3</sup>*JWK Corporation, Annandale, Virginia 22003, USA*

<sup>4</sup>*Vantage Partners, LLC, Brook Park, Ohio 44142, USA*

<sup>5</sup>*Cleveland State University, Cleveland, Ohio 44115, USA*

<sup>6</sup>*Ohio Aerospace Institute, Brook Park, Ohio 44142, USA*

 (Received 15 October 2018; revised manuscript received 8 February 2019; accepted 10 December 2019; published 20 April 2020)

Nuclear fusion reactions of D-D are examined in an environment comprised of high density cold fuel embedded in metal lattices in which a small fuel portion is activated by hot neutrons. Such an environment provides for enhanced screening of the Coulomb barrier due to conduction and shell electrons of the metal lattice, or by plasma induced by ionizing radiation ( $\gamma$  quanta). We show that neutrons are far more efficient than energetic charged particles, such as light particles ( $e^-$ ,  $e^+$ ) or heavy particles ( $p$ ,  $d$ ,  $\alpha$ ) in transferring kinetic energy to fuel nuclei (D) to initiate fusion processes. It is well known that screening increases the probability of tunneling through the Coulomb barrier. Electron screening also significantly increases the probability of large vs small angle Coulomb scattering of the reacting nuclei to enable subsequent nuclear reactions via tunneling. This probability is incorporated into the astrophysical factor  $S(E)$ . Aspects of screening effects to enable calculation of nuclear reaction rates are also evaluated, including Coulomb scattering and localized heating of the cold fuel, primary D-D reactions, and subsequent reactions with both the fuel and the lattice nuclei. The effect of screening for enhancement of the total nuclear reaction rate is a function of multiple parameters including fuel temperature and the relative scattering probability between the fuel and lattice metal nuclei. Screening also significantly increases the probability of interaction between hot fuel and lattice nuclei increasing the likelihood of Oppenheimer-Phillips processes opening a potential route to reaction multiplication. We demonstrate that the screened Coulomb potential of the target ion is determined by the nonlinear Vlasov potential and not by the Debye potential. In general, the effect of screening becomes important at low kinetic energy of the projectile. We examine the range of applicability of both the analytical and asymptotic expressions for the well-known electron screening lattice potential energy  $U_e$ , which is valid only for  $E \gg U_e$  ( $E$  is the energy in the center of mass reference frame). We demonstrate that for  $E \leq U_e$ , a direct calculation of Gamow factor for screened Coulomb potential is required to avoid unreasonably high values of the enhancement factor  $f(E)$  by the analytical—and more so by the asymptotic—formulas.

DOI: [10.1103/PhysRevC.101.044609](https://doi.org/10.1103/PhysRevC.101.044609)

**I. INTRODUCTION**

Electron screening is essential for efficient nuclear fusion reactions to occur. Screening effects on fusion reaction rates as measured in deuterated materials have been demonstrated to be important. The nuclear reaction rate includes two primary factors: the Coulomb scattering of the projectile nuclei on the target nuclei as well as nuclei tunneling through the Coulomb barrier. During elastic scattering of charged projectiles on a target nucleus, such as a deuteron, some of the energy of the projectile particle is transferred to the target nucleus, hence heating it. Depending on the projectile particle energy and

the efficiency of kinetic energy transfer during the scattering event, the target deuteron may become energetic enough to enable subsequent nuclear fusion reactions via tunneling through the Coulomb barrier. Electron screening may play a significant role in this process because of hot fuel interacting with lattice nuclei in the highly screened environment, as has been demonstrated in the companion experimental work reported in Steinetz *et al.* [1]. In the current work we analyze the electron screening effect on Coulomb scattering and the tunneling process involving charged projectiles. We then demonstrate the superior efficiency of the kinetic energy transfer by energetic neutrons on the target deuteron nuclei resulting in subsequent nuclear reactions. Such a process is a key ingredient in achieving and sustaining nuclear reactions.

\*Corresponding author: [vpines@wowway.com](mailto:vpines@wowway.com)

## II. NUCLEAR FUSION CROSS SECTION OF BARE NUCLEUS IONS

In the standard case of subbarrier quantum tunneling through the Coulomb barrier between positive nucleus ions, the nuclear fusion cross section of bare nucleus ions  $\sigma_{\text{bare}}(E)$  can be written [2] as

$$\sigma_{\text{bare}}(E) = \frac{S(E)}{E} \exp[-G(E)], \quad (1)$$

where  $E$  is the energy in the CM (center of mass) reference frame,  $G(E)$  is the Gamow factor, and  $S(E)$  [2,3] is the astrophysical  $S$ -factor containing the details of nuclear interactions. It is noted that the theoretical development proceeds in Gauss units (not SI). In the nonrelativistic case, the relation between energy  $E$  in the CM frame and the kinetic energy  $K_{1\infty}$  of the projectile nucleus ion in the laboratory (lab) frame takes the simple form

$$K_{1\infty} \equiv \frac{m_1 \vec{v}_{1\infty}^2}{2} = \left(1 + \frac{m_1}{m_2}\right) E. \quad (2)$$

In the lab frame, the target nucleus ion with mass  $m_2$  is at rest (i.e.,  $\vec{v}_2 = 0$ ), and the projectile nucleus ion with mass  $m_1$  has velocity  $\vec{v}_{1\infty}$  at infinity.

In the Wentzel-Kramers-Brillouin (WKB) approximation,  $G(E)$  involves the evaluation of the following integral [2]:

$$G(E) = \frac{2}{\hbar} \int_{r_0}^{r_{\text{ctp}}} [2\mu[U_C(r) - E]]^{1/2} dr. \quad (3)$$

Here,  $U_C(r)$  is the Coulomb potential energy (or the Coulomb barrier),  $U_C(r) = Z_1 e Z_2 e / r$  of a projectile nucleus with charge  $Z_1 e$  in the Coulomb field  $Z_2 e / r$  of target nucleus;  $\mu = m_1 m_2 / (m_1 + m_2)$  is the reduced mass of projectile and target nuclei;  $r_0 = (R_1 + R_2)$  is the classical distance of closest approach with nuclei (effective) radii  $R_1$  and  $R_2$ ; and  $r_{\text{ctp}}$  is the classical turning point, determined from the following expression:

$$E = U_C(r_{\text{ctp}}) \rightarrow r_{\text{ctp}} = Z_1 e \cdot Z_2 e / E. \quad (4)$$

Evaluation of the integral in Eq. (3) gives the standard expression for the Gamow factor [2], as derived in Eq. (6):

$$G_C(E) = \left(\frac{E_G}{E}\right)^{1/2} \left\{ \frac{2}{\pi} \cos^{-1} \left[ \sqrt{\frac{E}{V_C}} - \sqrt{\frac{E}{V_C} \left(1 - \frac{E}{V_C}\right)} \right] \right\}, \quad (5)$$

where  $V_C = Z_1 e \cdot Z_2 e / r_0$  is the full height of the Coulomb barrier,  $E_G = 2\mu c^2 (\pi \alpha Z_1 Z_2)^2$  is the Gamow energy, and  $\alpha = e^2 / \hbar c$ .

In the limit of  $\sqrt{E/V_C} \ll 1$  (which is usually the case), the Gamow factor reduces to the simple Sommerfeld expression [2,3]:

$$G_{C,\text{asymptotic}}(E) = \left(\frac{E_G}{E}\right)^{1/2} \left(1 - \frac{4}{\pi} \sqrt{\frac{E}{V_C}} + \dots\right) \rightarrow \left(\frac{E_G}{E}\right)^{1/2}. \quad (6)$$

## III. NUCLEAR FUSION WITH ELECTRON SCREENING

### A. Coulomb barrier screening by lattice electrons

In experiments with deuteron beams and deuterated targets, when target deuterium nuclei (D) were embedded in insulators and semiconductors [4,5], a relatively small enhancement of nuclear reaction rates was found for the  $D(d, p)T$  nuclear fusion reaction compared to reactions with gaseous  $D_2$  target experiments [6]. These enhancements of reaction rates for the  $D(d, p)T$  nuclear reaction in host insulators and semiconductors is naturally explained by the screening of interacting nuclei with static electron clouds localized in atomic shells of host materials [4]. Collectively, shell electrons are producing a negative screening potential for the projectile nucleus, effectively reducing the height and spatial extension of the Coulomb barrier between interacting nuclei [5].

However, much larger effects have been readily measured with deuterated metal targets (excluding the noble metals such as Cu, Ag, and Au) [5,7,8]. A large enhancement of the nuclear reaction rates for the  $D(d, p)T$  fusion reaction in host metals can be considered as the result of an additional dynamic screening by free-moving conduction electrons, which are readily concentrated near the positive ions [5]. These screening effects are collectively referred to as ‘‘lattice screening.’’

Electron screening of target nuclei either by atomic shell electrons or conduction electrons are usually both approximated by a negative uniform shift  $-U_e$  of the Coulomb barrier  $U_C(r)$ . Here  $U_e$  is the electron screening potential energy and is given by the simple formula [9]

$$U_e = \frac{Z_1 e Z_2 e}{\lambda_{\text{sc}}}, \quad (7)$$

where  $Z_1$  and  $Z_2$  are the atomic number of projectile and target nuclei, respectively, and  $\lambda_{\text{sc}}$  is the corresponding screening length. The standard derivation of Eq. (7) and the effect of electron screening can be straightforwardly estimated by recalculating the Gamow factor  $G(E)$  in Eq. (3) by replacing the Coulomb potential energy  $U_C(r)$  with the general expression for the screened Coulomb potential energy  $U_{C,\text{sc}(r)}$  [10]:

$$U_{C,\text{sc}(r)} = \frac{Z_1 e Z_2 e}{r} \exp\left(-\frac{r}{\lambda_{\text{sc}}}\right). \quad (8)$$

Since the radial distance  $r$  in Eq. (3) is smaller or equal to the classical turning point  $r_{\text{ctp}}$ , given by Eq. (4), which in turn is generally much smaller than the characteristic distance of electron cloud distribution from reacting nuclei, which is the corresponding screening length  $\lambda_{\text{sc}}$ , that is

$$r_0 \leq r \leq r_{\text{ctp}} \ll \lambda_{\text{sc}}, \quad (9)$$

one can expand  $\exp(-\frac{r}{\lambda_{\text{sc}}}) = (1 - \frac{r}{\lambda_{\text{sc}}})$  in Eq. (8) to find that the screened Coulomb potential energy  $U_{C,\text{sc}(r)}$  (the screened Coulomb barrier) can be rewritten [9] as

$$U_{C,\text{sc}(r)} = \frac{Z_1 e Z_2 e}{r} \left(1 - \frac{r}{\lambda_{\text{sc}}}\right) = \frac{Z_1 e Z_2 e}{r} - \frac{Z_1 e Z_2 e}{\lambda_{\text{sc}}} = U_C(r) - U_e, \quad (10)$$

TABLE I. Enhancement factor values for  $\text{ErD}_3$  at various energy levels.

$E$ eV	$f_{\text{direct}}(E)$ [Eq. (21)]	$f_{U_e}(E)$ [Eq. (17)]	$f_{U_e, \text{asymptotic}}(E)$ [Eq. (18)]	$\frac{f_{U_e}(E)}{f_{\text{direct}}(E)}$	$\frac{f_{U_e, \text{asymptotic}}(E)}{f_{\text{direct}}(E)}$
$\frac{1}{2}U_e$	$1.09 \times 10^{12}$	$2.36 \times 10^{13}$	$1.9 \times 10^{32}$	21.5	$1.7 \times 10^{20}$
$U_e$	$9.89 \times 10^5$	$3.09 \times 10^6$	$1.96 \times 10^{11}$	3	$2 \times 10^5$
$2U_e$	539	676	8286	1.25	15.4
$3U_e$	45.7	46.4	127	1.017	2.8

with the standard Coulomb barrier  $U_C(r)$  as

$$U_C(r) = \frac{Z_1 e Z_2 e}{r} \quad (11)$$

and the electron screening potential energy  $U_e$ , naturally determined [9] as

$$U_e = \frac{Z_1 e Z_2 e}{\lambda_{\text{sc}}}. \quad (12)$$

Therefore, the concept of an electron screening potential energy  $U_e$ , introduced above in Eqs. (7)–(11), can be theoretically justified if the classical turning point  $r_{\text{ctp}}$  is much smaller than the corresponding screening length  $\lambda_{\text{sc}}$ . This necessary condition, stated in Eq. (9), can be rewritten as

$$E \gg U_e, \quad (13)$$

using the definition of the classical turning point  $r_{\text{ctp}}$  given by Eq. (4).

Obviously for low energy,  $E \leq U_e$ , the concept of an electron screening potential energy  $U_e$  given by Eqs. (7)–(11) is not applicable, and the direct numerical evaluation of the Gamow factor  $G(E)$  in Eq. (3) with the screened Coulomb potential energy  $U_{C, \text{sc}(r)}$  from Eq. (8) is required.

It is well known [5,9] that the lowering of  $U_C(r)$  by  $U_e$  is equivalent to the increase of  $E$  by  $U_e$ , as can be seen in Eq. (3), namely,  $[U_C(r) - U_e] - E = U_C(r) - (E + U_e)$ . The uniform shift  $U_e$  is called the “electron screening potential energy” [5].

Therefore, the experimentally measured tunneling probability  $\sigma_{\text{exp}}(E)$  in the screened target at the ion energy  $E$  in the CM frame can be evaluated as the experimentally measured tunneling probability for bare ions collision at higher energy  $(E + U_e)$  [11]:

$$\sigma_{\text{exp}}(E) \equiv \sigma_{\text{screen}}(E) = \sigma_{\text{bare}}(E + U_e). \quad (14)$$

The experimental fusion cross-section  $\sigma_{\text{exp}}(E)$  can be written [11,12] as

$$\sigma_{\text{exp}}(E) = \sigma_{\text{bare}}(E) f(E), \quad (15)$$

which is essentially the definition of the enhancement factor  $f(E)$ .

From Eq. (1) the expression for an enhancement factor  $f_{U_e}(E)$  in the lattice potential approximation is found to be

$$f_{U_e}(E) = \frac{S(E + U_e)}{S(E)} \frac{E}{(E + U_e)} \exp[G_C(E) - G_C(E + U_e)]. \quad (16)$$

In the case of  $S(E + U_e) \cong S(E)$ , which is usually the general case, the enhancement factor  $f_{U_e}(E)$  can be finally written [5] as

$$f_{U_e}(E) = \frac{E}{(E + U_e)} \exp[G_C(E) - G_C(E + U_e)]. \quad (17)$$

In the limit of  $\sqrt{E N_C} \ll 1$ , Eq. (17) is further reduced to the following asymptotic formula [5,11,12]:

$$f_{U_e, \text{asymptotic}}(E) = \frac{E}{(E + U_e)} \exp\left[\frac{U_e}{2E} \left(\frac{E_G}{E}\right)^{1/2}\right], \quad (18)$$

following from Eq. (6).

For low energy (when  $E \leq U_e$ ) the concept of an electron screening potential energy  $U_e$  given by Eqs. (7)–(11) is not applicable, and the direct numerical evaluation is required. For the Gamow factor  $G_{\text{direct}}(E)$  in Eq. (3) with  $U_C(r) \rightarrow U_{C, \text{sc}}(r)$ ,

$$G_{\text{direct}}(E) \equiv G_{C, \text{sc}}(E) = \frac{2}{\hbar} \int_{r_0}^{r_{\text{ctp}}^*} \{2\mu[U_{C, \text{sc}}(r) - E]\}^{1/2} dr, \quad (19)$$

where  $r_{\text{ctp}}^*$  is the modified classical turning point determined numerically from the following equation:

$$U_{C, \text{sc}}(r_{\text{ctp}}^*) \equiv \frac{Z_1 e Z_2 e}{r_{\text{ctp}}^*} \exp\left(-\frac{r_{\text{ctp}}^*}{\lambda_{\text{sc}}}\right) = E, \quad (20)$$

where the screened Coulomb potential energy  $U_{C, \text{sc}}(r)$  is obtained from Eq. (8).

The enhancement factor in this case is obviously equal to

$$f_{\text{direct}}(E) = \exp[G_C(E) - G_{\text{direct}}(E)], \quad (21)$$

where  $G_C(E)$  is determined from Eq. (5).

Table I presents the calculated values of enhancement factors for deuterated erbium  $\text{ErD}_3$  for various levels of energy of interest. Note that  $U_e$  was calculated using Eqs. (46) or (54) noted below and was found to be  $U_e = 347$  eV.

Note, for example, that the value of  $3U_e$  corresponds to 2 keV kinetic energy of the projectile in the lab frame, illustrating that the analytical formula for  $f_{U_e}(E)$  is valid, but the asymptotic formula for the enhancement factor is still inappropriate. Since the electron screening effect becomes important at low kinetic energy of the projectile, direct numerical calculation of the Gamow factor is required for accurate results.

The above equations show a sharp rise in enhancement factor  $f(E)$  for deuterium interaction with host metals, especially at moderately low deuteron energies. The enhancement factor

$f(E)$  further increases with  $Z$  and with decreasing projectile energy. This may enable Oppenheimer-Phillips stripping reactions resulting in the production of energetic protons and neutrons, and a possible route for multiplication. Such Oppenheimer-Phillips stripping reactions appear to have been observed in the companion experimental work reported in Steinetz *et al.* [1].

*Measured  $U_e$  for select targets.* The experimental values for electron screening potential energies  $U_e$  are as follows:  $U_e = 25 \pm 15$  eV for gaseous targets [6], and  $U_e = 39\text{--}52$  eV for deuterated insulators and semiconductors targets [4,5,7]. However, for deuterated metal targets much larger values of electron screening potential energies  $U_e$  are measured [5,7,8], ranging from  $U_e = 180 \pm 40$  eV (Be) to  $800 \pm 90$  eV (Pd). The exclusion is observed for deuterated noble metal targets [5,7,8], namely  $U_e = 43 \pm 20$  eV (Cu),  $U_e = 23 \pm 10$  eV (Ag), and  $U_e = 61 \pm 20$  eV (Au).

Theoretical values for  $U_e$ , considering screening by static electron clouds localized in atomic shells of host materials, that are calculated in the adiabatic limit utilizing differences in atomic binding energies [4], correlate well with experimentally measured values for  $U_e$  in gaseous targets as well as in deuterated insulator and semiconductor targets [4,5,7,8].

In contrast, theoretically calculated values of screening potential energies  $U_e$  by static electron clouds in atomic shells of host metals, are almost one order of magnitude smaller [4] than values of electron screening potential energies  $U_e$  experimentally measured for deuterated alkaline metal targets [5,7,8]. These discrepancies obviously require different physical mechanisms for theoretical clarification of experimental results. The novel physical mechanism, which takes into account the presence of quasifree moving conduction electrons in metals as an additional source for screening of interacting nuclei [5], will be discussed in Sec. III C.

### B. Coulomb barrier screening by plasma particles

In deuterated materials exposed to ionizing radiation ( $\gamma$  quanta or energetic electron  $e$  beam) dense plasma channels are created inside an irradiated sample comprising nonequilibrium two-temperature plasma with free moving hot electrons and free-moving cold deuteron ions.

Energetic electrons in plasma cannot create a bound state with deuteron ions, because the mean kinetic energy of hot electrons ( $\bar{K}_e \sim kT_e$ ) is much larger than the Coulomb interaction ( $\bar{U}_{ie} \sim q_i q_e / \bar{r}$ ) between them [13]:

$$\bar{K}_e \gg |\bar{U}_{ie}|. \quad (22)$$

The inequality in Eq. (22) represents the necessary condition for plasma existence and also can be written as

$$kT_e \gg e^2 n^{1/3}, \quad (23)$$

using the obvious fact that the mean distance  $\bar{r}$  between ions is of the order of  $n^{-1/3}$ :

$$\bar{r} \sim n^{-1/3}. \quad (24)$$

Introducing the electron Debye length  $\lambda_{De}$ , which is defined as

$$\lambda_{De} = \left( \frac{kT_e}{4\pi e^2 n} \right)^{1/2}, \quad (25)$$

Eq. (23) is rewritten with the help of Eq. (24) as

$$\lambda_{De}^2 \gg \frac{\bar{r}^2}{4\pi} \rightarrow \lambda_{De} > \frac{\bar{r}}{\sqrt{4\pi}} \cong 0.28\bar{r}. \quad (26)$$

Equation (26) indicates that in plasma the electron Debye length  $\lambda_{De}$  is larger in order of magnitude than the mean distance  $\bar{r}$  between ions.

It also follows from Eqs. (24) and (26) that the number of electrons in the electron Debye sphere  $N_{De}$  in plasma is much larger than 1 [13]:

$$N_{De} \sim n \left( \frac{4\pi}{3} \lambda_{De}^3 \right) \gg 1. \quad (27)$$

Therefore, the statement  $\lambda_{De} > 0.28\bar{r}$  as given by Eq. (26) and the equivalent statement  $N_{De} \gg 1$  as given by Eq. (27) follow from the plasma existence necessary requirement of  $\bar{K}_e \gg |\bar{U}_{ie}|$ , which is expressed by Eq. (22).

The undisturbed plasma in plasma channels is electroneutral, with the total electric charge density  $Q_0$  being equal to zero in each unit volume:

$$Q_0 = q_i n_{i0} + q_e n_{e0} = 0, \quad (28)$$

where  $n_{i0}$  is the undisturbed mean ion number density,  $n_{e0}$  is the undisturbed mean electron number density,  $q_i$  is the ion electrical charge, and  $q_e$  is the electron electrical charge. It follows from Eq. (28) that the electron and ion undisturbed number densities  $n_{e0}$  and  $n_{i0}$ , respectively, are equal to each other if  $q_i = -q_e = e$ :

$$Q_0 = q_i \cdot n_{i0} + q_e \cdot n_{e0} = 0 \rightarrow n \equiv n_{e0} = n_{i0}. \quad (29)$$

However, the long-range Coulomb forces between ions in the plasma act at distances that are much larger than the mean distance  $\bar{r}$  between plasma particles. The interaction between any two charged ions at such distances is influenced by the presence of a large number of charged particles. Consequently, the resulting effective field is collectively produced by many charged particles and naturally described by the self-consistent Vlasov field, which is not a random one, but macroscopically certain; that is, not causing the entropy of the system to increase [13,14].

In accord with the above description, each ion in the plasma can be considered as surrounded by a spherically symmetrical (on average) charged ion cloud with nonuniform charge density distribution  $Q(r)$ :

$$Q(r) = q_i n_i(r) + q_e n_e(r), \quad (30)$$

where  $r$  is the distance from the ion (located at  $r = 0$ ). Here  $n_e(r)$  is the electron number density and  $n_i(r)$  is the ion number density, both distributed in the self-consistent Vlasov potential field  $\phi(r)$  around the ion in consideration.

Since in the Vlasov field  $\phi(r)$  the potential energy of an electron is  $q_e \phi(r)$  and of the ion is  $q_i \phi(r)$ , the corresponding electron number density  $n_e(r)$  and ion number density  $n_i(r)$  are both given by the corresponding Boltzmann's distribution [13,14]:

$$n_e(r) = n_{e0} \exp \left[ -\frac{q_e \phi(r)}{kT_e} \right], \quad n_i(r) = n_{i0} \exp \left[ -\frac{q_i \phi(r)}{kT_i} \right], \quad (31)$$

where  $T_e$  and  $T_i$  are the electron and ion temperatures, respectively. Here  $n_{e0}$  and  $n_{i0}$  are the mean electron and ion number densities in undisturbed plasma.

The Vlasov potential  $\phi(r)$  in the ion cloud around any considered ion obeys the nonlinear electrostatic Poisson's equation (the Vlasov equation):

$$\nabla^2 \phi = \frac{1}{r^2} \frac{\partial}{\partial r} \left[ r^2 \frac{\partial \phi(r)}{\partial r} \right] = -4\pi Q(r) = -4\pi Q[\phi(r)], \quad (32)$$

where the total electric charge density  $Q(r)$  is the nonlinear function in  $\phi(r)$ , as given by Eq. (30) together with Eq. (31).

The solution of the Vlasov equation, Eq. (32), should be used in the evaluation of the Gamow factor in Eq. (3) for the screened Coulomb barrier  $U_{C,sc}$ . For the projectile nucleus with charge  $+e$  in the Vlasov potential field  $\phi(r)$  of target nucleus with charge  $q_i = +e$ , the screened Coulomb barrier  $U_{C,sc}$  by definition is

$$U_{C,sc} \equiv e\phi(r). \quad (33)$$

At large distance from the considered ion (located at  $r = 0$ ), the Vlasov field goes to zero  $\phi(r \rightarrow \infty) \rightarrow 0$ , since it describes the deviation from reference potential of unperturbed plasma. Thus

$$n_e(r \rightarrow \infty) \rightarrow n \equiv n_{e0} \text{ and } n_i(r \rightarrow \infty) \rightarrow n \equiv n_{i0}. \quad (34)$$

As the undisturbed plasma is electroneutral, the total electric charge density  $Q_0$  is equal to zero in each unit volume:

$$Q(r \rightarrow \infty) \rightarrow Q_0 = q_i n_{i0} + q_e n_{e0} = 0 \rightarrow n \equiv n_{e0} = n_{i0} \quad (35)$$

[see Eqs. (28) and (29)].

Since at large distance  $r$  from the ion (located at  $r = 0$ ), the Vlasov potential  $\phi(r)$  is small, the ion and electron charge density distributions can be reduced to linear expressions in term of  $\phi(r)$ :

$$\begin{aligned} n_e(r) &= n_{e0} \left( 1 - \frac{q_e}{kT_e} \phi(r) \right) \quad \text{and} \\ n_i(r) &= n_{i0} \left( 1 - \frac{q_i}{kT_i} \phi(r) \right), \end{aligned} \quad (36)$$

leading to a linear expression in  $\phi(r)$  for the total charge density  $Q[\phi(r)]$ :

$$Q[\phi(r)] = Q_0 - \left( \frac{q_i^2 n_{i0}}{kT_i} + \frac{q_e^2 n_{e0}}{kT_e} \right) \phi(r), \quad Q_0 = 0. \quad (37)$$

Substitution of Eq. (37) into Eq. (32) gives the linearized electrostatic Poisson's equation (Debye equation) for the Vlasov potential  $\phi(r)$  [13]:

$$\frac{1}{r^2} \frac{\partial}{\partial r} \left( r^2 \frac{\partial \phi(r)}{\partial r} \right) = \frac{1}{\lambda_D^2} \phi(r), \quad (38)$$

where  $\lambda_D$  is the Debye screening length in two-component, two-temperature plasma [15]:

$$\lambda_D^{-2} = \lambda_{Di}^{-2} + \lambda_{De}^{-2}, \quad (39)$$

where  $\lambda_{Di}$  and  $\lambda_{De}$  are the ion and electron Debye lengths, respectively. They are defined as

$$\begin{aligned} \lambda_{Di} &= \left( \frac{kT_i}{4\pi n_{i0} e^2} \right)^{1/2} \quad \text{and} \\ \lambda_{De} &= \left( \frac{kT_e}{4\pi n_{e0} e^2} \right)^{1/2}. \end{aligned} \quad (40)$$

If the electron temperature  $T_e$  is much higher than the ion temperature  $T_i$  (i.e., hot electrons and cold ions), then the Debye screening length  $\lambda_D$  for two-component, two-temperature plasma is determined by the ion Debye length  $\lambda_{Di}$ :

$$T_e \gg T_i \rightarrow \lambda_D = \lambda_{Di} = \left( \frac{kT_i}{4\pi n_{i0} e^2} \right)^{1/2}, \quad (41)$$

as it follows from Eqs. (39) and (40).

Near the ion with charge  $q_i = +e$  (located at  $r = 0$ ), the Vlasov potential  $\phi(r)$  reduces to the Coulomb potential  $q_i/r$ , generated by this ion:

$$\phi(r \rightarrow 0) \rightarrow \frac{q_i}{r}. \quad (42)$$

The exact solution of the Debye equation, Eq. (38), for the Debye potential  $\phi_D(r)$  that satisfies the boundary condition expressed by Eq. (42), takes the following simple form known as the Debye potential:

$$\phi_D(r) = \frac{q_i}{r} \exp\left(-\frac{r}{\lambda_D}\right). \quad (43)$$

The usual approximation of the Vlasov potential  $\phi(r)$  that obeys the nonlinear equation Eq. (32) by the linear Debye potential  $\phi_D(r)$  is expressed by Eq. (43) with the correct boundary condition from Eq. (42), which is extensively used in the nonlinear theory of plasma sheath [15,16].

This approximation can also be used to obtain the analytical expression for the plasma-screened Coulomb barrier  $U_{C,sc}$ . The Debye potential energy  $U_D(r)$  of the projectile nucleus with charge  $+e$  in the Debye potential field  $\phi_D(r)$  of the target nucleus with charge  $q_i = +e$ , given by Eq. (43), by definition is as follows:

$$U_{C,sc} \equiv U_V(r) = e\phi(r) \approx U_D = e\phi_D(r) = \frac{e^2}{r} \exp\left(-\frac{r}{\lambda_D}\right). \quad (44)$$

In summary, the correct expression for the screened Coulomb barrier  $U_{C,sc}$  is determined by the Vlasov potential and not by its linearized version, the Debye potential, and the Vlasov potential is valid at any temperature. The Vlasov potential can be obtained by direct numerical solution of the nonlinear equation, Eq. (32), with the total electric charge density  $Q(r)$  given by Eqs. (30) and (31). Alternatively, as commonly done in an evaluation of the nonlinear plasma sheath problem, it is linearized to the Debye potential given by Eq. (43), with the correct boundary condition Eq. (42), to merge with the Coulomb potential near the bare ion.

In dense nonequilibrium two-temperature plasma channels created in deuterated metal by  $\gamma$ -ionizing radiation, the electron temperature  $T_e$  is much higher than ion temperature  $T_i$ ,

and therefore the Debye screening length  $\lambda_D$  is determined mainly by the ion Debye length  $\lambda_{Di}$ , as it follows from Eqs. (39) and (40). Therefore, the Debye screening length  $\lambda_D$  as given by

Eq. (41) converts to

$$T_e \gg T_i \rightarrow \lambda_D = \lambda_{Di} = \left( \frac{kT_i}{4\pi n_{i0} e^2} \right)^{1/2} = 4.15 \times 10^{-10} \text{ cm}, \quad (45)$$

since in deuterated erbium  $\text{ErD}_3$  exposed to  $\gamma$ -ionizing radiation  $n_{i0} = n_{e0} = 8 \times 10^{22} \text{ cm}^{-3}$  and  $T_i = 293 \text{ K}$  (room temperature). Also, the plasma-particle screening potential energy  $U_e$ , which is given by Eq. (12) for deuterated erbium  $\text{ErD}_3$ , becomes equal to

$$U_e = \frac{e^2}{\lambda_D} = 347 \text{ eV}, \quad (46)$$

with  $\lambda_D$  from Eq. (45).

### C. Coulomb barrier screening by conduction electrons in metal lattice

In order to theoretically explain the high values of electron screening potential  $U_e^{\text{exp}}$  experimentally measured for deuterated alkaline metal targets [5,7,8], it was suggested in [5] to take into account the presence of quasi-free moving conduction electrons in metals for screening of interacting nuclei. Indeed, when atoms are tightly packed, such as in solid host metals, wave functions of valence electrons of individual atoms are overlapped, acquiring a considerable kinetic energy  $\bar{K}_{e,\text{degeneracy}}$  due to quantum degeneracy. The Fermi repulsion is large enough to liberate valence electrons from individual atoms into a sea of conduction electrons, since they are identical particles and are truly indistinguishable.

This electron degeneracy energy  $\bar{K}_{e,\text{degeneracy}}$ , called the Fermi energy  $\varepsilon_F$ , can be straightforwardly estimated from the Heisenberg uncertainty relation:

$$\Delta p_e \Delta r \sim \hbar. \quad (47)$$

The root-mean-square of electron momentum  $p_e \equiv \sqrt{\langle p_e^2 \rangle}$  is equal to momentum uncertainty  $\Delta p_e$ , if  $\langle p_e \rangle = 0$ :

$$p_e = \Delta p_e = \sqrt{\langle p_e^2 \rangle} = \sqrt{\langle p_e^2 \rangle} = \sqrt{\langle p_e^2 \rangle} \quad (48)$$

and  $\Delta r$  is of the order of the characteristic distance between electrons  $\bar{r}$ , which in turn is of the order of  $n_e^{-1/3}$ :

$$\Delta r \sim \bar{r} \cong n_e^{-1/3}, \quad (49)$$

where  $n_e$  is the electron number density. The value of  $p_e$  is obtained from Eqs. (32)–(34):

$$p_e \sim \frac{\hbar}{\bar{r}} \cong \hbar n_e^{1/3}. \quad (50)$$

Then the Fermi energy  $\varepsilon_F$  is estimated to be

$$\bar{K}_{e,\text{degeneracy}} \equiv \varepsilon_F \sim \frac{p_e^2}{m_e} \cong \frac{\hbar^2}{m_e} n_e^{2/3}. \quad (51)$$

More precise calculation of the Fermi energy  $\varepsilon_F$  (for degenerate electron gas) is given by the following expression [13]:

$$\varepsilon_F = \frac{(3\pi^2)^{2/3} \hbar^2}{2 m_e} n_e^{2/3} = 4.78 \frac{\hbar^2}{m_e} n_e^{2/3}. \quad (52)$$

It was considered in [5] that differences between the Fermi-Dirac and classical (Boltzmann) distributions of the conduction electrons may be expected to be negligible for the electron screening at room temperature [5,17]. In that simplified model [5], deuteron ions together with metal conduction electrons were treated as a one-component equilibrium classical plasma, which comprises metallic quasifree moving conduction electrons (providing plasma screening), and singly charged localized deuteron ions (not contributing to plasma screening). The Debye screening length in one-component, equilibrium ( $T_e = T_i$ ) classical (Boltzmann) plasma that approximates the screening by conduction electrons,  $\lambda_{De,c}$ , is then reduced to the electron Debye screening length  $\lambda_{De}$ :

$$\lambda_{De,c} = \lambda_{De} = \left( \frac{kT_e}{4\pi n_{e0} e^2} \right)^{1/2}. \quad (53)$$

For deuterated erbium  $\text{ErD}_3$  with material parameters  $n_{e0} = n_{i0} = 8 \times 10^{22} \text{ cm}^{-3}$  and  $T_e = 293 \text{ K}$  (room temperature), Eq. (53) gives  $\lambda_{De,c} = 4.15 \times 10^{-10} \text{ cm}$ . Therefore, the conduction-electron screening potential energy  $U_e$ , which is given by Eq. (12) for deuterated erbium  $\text{ErD}_3$ , is equal to

$$U_e = \frac{e^2}{\lambda_{De,c}} = 347 \text{ eV}, \quad (54)$$

with  $\lambda_{De,c}$  from Eq. (53). It is obvious that a much better estimate of  $U_{e,c}$  can be achieved with Fermi-Dirac statistics for the description of conduction electrons rather than with the classical (Boltzmann) statistics. It is noted that the screening potential values calculated for plasma and conduction electrons are identical, although for different reasons. Indeed, plasma formation may also contribute to screening in nonmetal targets, e.g., in dense deuterium gas irradiated by ionizing radiation.

### D. Screening of reacting hydrogen isotope nuclei by atomic shell (bound) electrons in deuterated metals

The screening of ions by atomic shell (bound) electrons is modeled by the Thomas-Fermi model. The Wentzel-Thomas-Fermi screened Coulomb atomic potential (energy) is

$$V_{C,\text{sc}}(r) = \frac{Z_1 e (Z_2 e)}{r} \exp\left(-\frac{r}{\lambda_{\text{TF}}}\right), \quad (55)$$

where  $Z_1$  and  $Z_2$  are the atomic numbers of projectile and target (host) nuclei, respectively, and, for instance, the modified (to better fit experimental data) Thomas-Fermi screening length  $\lambda_{\text{TF}}$  (atom size) by atomic shell electrons of the host material is given by the following relation [11]:

$$\lambda_{\text{TF}} = \frac{1.4a_0}{Z^{1/3}}, \quad (56)$$

where  $a_0$  is the Bohr radius,  $a_0 = 5.29 \times 10^{-9} \text{ cm}$  and  $Z$  is the atomic number of the host material.

#### IV. GENERAL SCREENING CASE FOR REACTING HYDROGEN ISOTOPE NUCLEI

In the general case, taking into account possible simultaneous screening of reacting hydrogen isotope nuclei by atomic shell electrons of the host material and by conduction electrons, or by atomic shell electrons of the host material and plasma electrons, the total screening potential energy  $U_{e,sc}$  can be estimated [18] as

$$U_{e,sc} = \frac{e^2}{\lambda_{sc}}, \quad (57)$$

where the screening length  $\lambda_{sc}$  is given by one of the following general relations [18]:

$$\lambda_{sc}^{-2} = \lambda_{TF}^{-2} + \lambda_{De,c}^{-2} \quad \text{or} \quad \lambda_{sc}^{-2} = \lambda_{TF}^{-2} + \lambda_D^{-2}, \quad (58)$$

where  $\lambda_{TF}$  is the modified Thomas-Fermi screening length by atomic shell electrons of host material,  $\lambda_{De,c}$  is the screening length by conduction electrons, and  $\lambda_D$  is the Debye screening length in plasma.

Since the inverse square of screening length  $\lambda_{TF}^{-2}$ ,  $\lambda_{De,c}^{-2}$ , or  $\lambda_D^{-2}$  is proportional to the corresponding electron number density, the derivation of Eqs. (57) and (58) is similar to the derivation of Eqs. (39) and (40), as the summation of electron number densities was used in both of them to contribute to the total charge density in electrostatic Poisson's equation for screened Coulomb interaction potential.

#### V. COULOMB SCATTERING ON TARGET NUCLEI

##### A. Light particles elastic Coulomb scattering ( $e^-$ , $e^+$ )

Coulomb scattering of energetic projectile particles on target nuclei is the principle process associated with fusion reactions of interest. Fusion nuclear events are more likely under the condition of large-angle scattering, which brings the reacting ions to the classical distance of closest approach to successfully tunnel through the Coulomb barrier. However, the elastic scattering at a small angle dominates the Coulomb scattering interaction. Generally, the electron screening of the Coulomb barrier could significantly reduce the small-angle elastic scattering, increasing the probability of large-angle scattering and correspondingly successful nuclear fusion events. Elastic scattering studies on Coulomb scattering of energetic projectiles on target nuclei are analyzed and extended to include the electron screening by plasma electrons as well as by conduction electrons in deuterated metals. It is also found that the kinetic energy transfer (kinetic heating) to fuel nuclei is most effective by energetic neutrons, such as  $\gamma$  induced photoneutrons.

The Coulomb scattering of relativistic projectile electrons on target atoms (absorbing medium) characterizes by the projectile electron-target atom differential cross section  $d\sigma/d\Omega|_{e-a}$ , which is determined as the sum of the projectile electron-target nucleus differential cross section  $d\sigma/d\Omega|_{e-N}$  and the projectile electron-target orbital electron differential cross section  $d\sigma/d\Omega|_{e-e}$  multiplied by  $Z$  (the atomic number of target atoms). It is given by the following relation

[14,19,20]:

$$\begin{aligned} \frac{d\sigma}{d\Omega}\Big|_{e-a} &= \frac{d\sigma}{d\Omega}\Big|_{e-N} + Z \frac{d\sigma}{d\Omega}\Big|_{e-e} \\ &= \frac{D_{e-a}^2 (1 - \frac{\beta^2}{2} (1 - \cos \theta))}{[2(1 - \cos \theta) + \theta_{\min}^2]^2}, \end{aligned} \quad (59)$$

where  $\theta$  is the electron scattering angle,  $\beta = v_e/c$  (with  $v_e$  being the velocity of the projectile electron and  $c$  being the speed of light) and  $\theta_{\min}$  is the atomic screening parameter defined as

$$\theta_{\min} = \frac{\hbar/\lambda_{TF}}{p_e}, \quad (60)$$

where  $\hbar$  is the reduced Planck constant and  $\lambda_{TF}$  is the modified Thomas-Fermi target atomic radius given by Eq. (56). The electron momentum  $p_e$  is determined by the following relations:

$$p_e = \frac{E_e}{c} \left( 1 + \frac{2m_e c^2}{E_e} \right)^{1/2}, \quad (61)$$

where  $E_e = E_{e,\text{tot}} - m_e c^2$  is the kinetic energy of projectile electron ( $E_{e,\text{tot}}$  is the total energy of projectile electron and  $m_e$  is the electron mass).

Equation (59) was derived in the first Born approximation to the Dirac equation for the Wentzel-Thomas-Fermi screened Coulomb atomic potential (energy) given by Eq. (55):

$$V_{C,sc}(r) = \frac{e(Ze)}{r} \exp\left(-\frac{r}{\lambda_{TF}}\right), \quad (62)$$

where  $\lambda_{TF}$  is the Thomas-Fermi screening length (atom size) by atomic shell electrons of host material given by Eq. (56).

The projectile electron-target atom elastic scattering characteristic distance  $D_{e-a}$  is determined from the following relation:

$$D_{e-a}^2 = D_{e-N}^2 + Z D_{e-e}^2, \quad (63)$$

where the projectile electron-target nucleus characteristic scattering distance  $D_{e-N}$  is determined by

$$\begin{aligned} D_{e-N} &= \frac{Z e^2}{\gamma m_e v_e^2 / 2} = \frac{2Z r_e \sqrt{1 - \beta^2}}{\beta^2} \\ &= \frac{2Z e^2}{\beta E_e (1 + 2m_e c^2 / E_e)^{1/2}} \end{aligned} \quad (64)$$

with  $\gamma = 1/\sqrt{1 - \beta^2}$ , and the projectile electron-target orbital electron characteristic scattering distance  $D_{e-e}$  is given by Eq. (63) with  $Z = 1$ .

Here  $r_e = e^2/m_e c^2$  is the classical radius of an electron  $r_e = 2.82 \text{ fm} = 2.82 \times 10^{-13} \text{ cm}$ . Substitution of  $D_{e-N}$  from Eq. (64) and  $D_{e-e}$  into Eq. (63) yields

$$D_{e-a} = \frac{2r_e \sqrt{Z(Z+1)}}{\gamma \beta^2} = \frac{2e^2 \sqrt{Z(Z+1)}}{\beta E_e (1 + 2m_e c^2 / E_e)^{1/2}}. \quad (65)$$

The total cross section  $s_{e-a}$  is obtained by integrating over  $d\Omega$  the differential cross section for projectile electrons

scattering on target atoms from Eq. (59):

$$\sigma_{e-a} = \int \left. \frac{d\sigma}{d\Omega} \right|_{e-a} d\Omega = \frac{\pi D_{e-a}^2}{\theta_{\min}^2} \times \left[ \left( \frac{4 + \beta^2 \theta_{\min}^2}{4 + \theta_{\min}^2} \right) - \frac{\beta^2 \theta_{\min}^2}{4} \ln \left( \frac{4}{\theta_{\min}^2} - 1 \right) \right], \quad (66)$$

where  $\theta_{\min} = (\hbar/p_e)\lambda_{\text{TF}}^{-1}$ , is given by Eq. (60). The expression for  $s_{e-N}$  follows from Eq. (66) with the obvious substitution  $D_{e-a}^2 \rightarrow D_{e-N}^2$ .

For  $E_e = 2$  MeV and  $m_N = m_d$  (deuteron mass), the numerical value for  $s_{e-d}$  is

$$\sigma_{e-d} = \int \left. \frac{d\sigma}{d\Omega} \right|_{e-d} d\Omega \approx \frac{\pi D_{e-d}^2}{\theta_{\min}^2} = \frac{4\pi e^4 \lambda_{\text{TF}}^2}{\hbar^2 c^2 \beta^2} = 38.41 \text{ kb} \quad (67)$$

since  $\pi D_{e-d}^2 = 45.1$  mb, but  $\theta_{\min}^2 = (\hbar/p_e)^2 \lambda_{\text{TF}}^{-2} = 1.17 \times 10^{-6}$ .

The target nucleus recoil energy can be found from the conservation of the total momentum in the elastic projectile electron-target nucleus scattering process

$$\vec{p}_N = \vec{p}_e - \vec{p}'_e, \quad (68)$$

where  $\vec{p}_N$  is the target nucleus recoil momentum,  $\vec{p}_e$  is the momentum of the incident electron, and  $\vec{p}'_e$  is the momentum of the scattered electron. Since in elastic scattering  $p_e = |\vec{p}_e| \approx |\vec{p}'_e|$  (for the reason that small-angle scattering is the most probable event), it follows from Eq. (68) that

$$p_N^2 = \vec{p}_N^2 = \vec{p}_e^2 + \vec{p}'_e^2 - 2p_e p'_e \cos \theta \approx 2p_e^2 (1 - \cos \theta), \quad (69)$$

where  $\theta$  is the scattering angle. Correspondingly, it follows from Eq. (69) with the help of Eq. (61) that the target nucleus recoil energy  $E_N(\theta)$  is

$$\begin{aligned} E_N(\theta) &= \frac{p_N^2}{2m_N} \approx \frac{p_e^2}{m_N} (1 - \cos \theta) \\ &= \frac{E_e^2}{m_N c^2} \left( 1 + \frac{2m_e c^2}{E_e} \right) (1 - \cos \theta), \end{aligned} \quad (70)$$

where  $E_e = E_{e,\text{tot}} - m_e c^2$  is the kinetic energy of projectile electron ( $E_{e,\text{tot}}$  is the total energy of projectile electron, and  $m_e$  and  $m_N$  are the electron and nucleus mass, respectively).

The mean target nucleus recoil energy  $\bar{E}_N$  in single elastic projectile electron-nucleus (target) collision is obtained by averaging of  $E_N(\theta)$  over  $d\Omega$ :

$$\bar{E}_N = \frac{\int E_N(\theta) d\sigma / d\Omega|_{e-N} d\Omega}{\int d\sigma / d\Omega|_{e-N} d\Omega}. \quad (71)$$

Substitution of  $d\sigma / d\Omega|_{e-N}$  into Eq. (71) and taking the integral yields the expression for the mean target nucleus recoil energy  $\bar{E}_N$  in single elastic projectile electron-nucleus (target) collision:

$$\begin{aligned} \bar{E}_N &= \frac{\hbar^2}{m_N \lambda_{\text{TF}}^2} \\ &\times \frac{\left\{ (2 + \alpha)(1 + \alpha\beta^2) \ln \left( \frac{2+\alpha}{\alpha} \right) - 2[1 + (1 + \alpha)\beta^2] \right\}}{2(2 + \alpha\beta^2) - \alpha(2 + \alpha)\beta^2 \ln \left( \frac{2+\alpha}{\alpha} \right)}, \end{aligned} \quad (72)$$

where  $\alpha = \theta_{\min}^2/2$ ,  $\beta = v_e/c$ . For  $E_e = 2$  MeV and  $m_N = m_d$  (deuteron mass), the numerical value for the mean target nucleus recoil energy  $\bar{E}_N = \bar{E}_d$  in single elastic projectile electron-target deuteron nucleus collision is

$$\bar{E}_d = 24.75 \text{ meV}. \quad (73)$$

### B. Heavy particle elastic Coulomb scattering ( $p, d, \alpha$ )

The Coulomb scattering of the heavy projectile particles on target nuclei is characterized by the differential cross section of the heavy projectile particles and nuclei, which is given by Eq. (59) for the obvious substitution  $D_{e-a}^2 \rightarrow D_{p-N}^2$  with  $\beta = v_p/c$ , and

$$\theta_{\min,p} = \frac{\hbar/\lambda_{\text{TF}}}{p_p} = \frac{\hbar/\lambda_{\text{TF}}}{\sqrt{2m_p E_p}}, \quad (74)$$

where  $p_p = \sqrt{2m_p E_p}$  is the projectile momentum and  $m_p$  and  $E_p$  are the projectile mass and kinetic energy, respectively.

The projectile particle-target nucleus characteristic scattering distance  $D_{p-N}$  is determined by

$$D_{p-N} = \frac{z_p Z_N e^2}{E_p}, \quad (75)$$

where  $z_p$  is the projectile particle atomic number ( $z_p = 1$  for the proton and deuteron projectile,  $z_p = 2$  for the  $\alpha$  projectile) and  $Z_N$  is the target nucleus atomic number.

The total cross section  $\sigma_{p-N}$  is obtained from Eq. (66) with the obvious substitution  $D_{e-a}^2 \rightarrow D_{p-N}^2$  and with  $\beta \rightarrow \beta_p \ll 1$ , since the heavy projectiles are nonrelativistic:

$$\begin{aligned} \sigma_{p-N} &= \frac{\pi D_{p-N}^2}{\theta_{\min,p}^2} \left( 1 + \frac{\theta_{\min,p}^2}{4} \right)^{-1} \rightarrow \frac{\pi D_{p-N}^2}{\theta_{\min,p}^2} \\ &= \frac{2\pi m_p e^4 z_p^2 Z_N^2 \lambda_{\text{TF}}^2}{\hbar^2 E_p} \end{aligned} \quad (76)$$

since  $\theta_{\min,p} = \hbar/(\lambda_{\text{TF}} p_p) \ll 1$ ,  $\lambda_{\text{TF}} = 1.4 a_0 Z_N^{-1/3}$ , and  $p_p = \sqrt{2m_p E_p}$ .

For a proton projectile with  $E_p = 3$  MeV and deuteron target nucleus ( $m_N = m_d$ ), the numerical value for  $\sigma_{p-D}$  (total scattering cross section) is

$$\begin{aligned} \sigma_{p-D} &= \int \left. \frac{d\sigma}{d\Omega} \right|_{p-D} d\Omega \approx \frac{\pi D_{p-D}^2}{\theta_{\min,p}^2} \\ &= \frac{2\pi m_p e^4 \lambda_{\text{TF}}^2}{\hbar^2 E_p} = 5.76 \text{ Mb}. \end{aligned} \quad (77)$$

For a deuteron projectile with  $E_d = 3$  MeV and deuteron target nucleus ( $m_N = m_d$ ), the numerical value for  $\sigma_{d-D}$  is

$$\begin{aligned} \sigma_{d-D} &= \int \left. \frac{d\sigma}{d\Omega} \right|_{d-D} d\Omega \approx \frac{\pi D_{d-D}^2}{\theta_{\min,d}^2} \\ &= \frac{2\pi m_d e^4 \lambda_{\text{TF}}^2}{\hbar^2 E_d} = 11.51 \text{ Mb}, \end{aligned} \quad (78)$$

whereas for deuteron projectile with  $E_d = 10$  keV and deuteron target nucleus ( $m_N = m_d$ ), the numerical value for



$\sigma_{d-D}$  is as follows:

$$\begin{aligned}\sigma_{d-D} &= \int \frac{d\sigma}{d\Omega} \Big|_{d-D} d\Omega \approx \frac{\pi D_{d-D}^2}{\theta_{\min,d}^2} \\ &= \frac{2\pi m_d e^4 \lambda_{TF}^2}{\hbar^2 E_d} = 3.45 \text{ Gb.}\end{aligned}\quad (79)$$

The relative probability  $P_{sc}(\pi/2 \leq \theta \leq \pi)$  to scatter in the back hemisphere ( $\pi/2 \leq \theta \leq \pi$ ) is equal to

$$P_{sc}(\pi/2 \leq \theta \leq \pi) = \frac{1}{\sigma_{d-D}} \int_{\pi/2}^{\pi} d\sigma/d\Omega \Big|_{d-D} 2\pi \sin\theta d\theta. \quad (80)$$

For a deuteron projectile with  $E_d = 3$  MeV and deuteron target nucleus ( $m_N = m_d$ ), the numerical value of  $P_{sc}(\pi/2 \leq \theta \leq \pi)$  for screening by a deuteron shell electron ( $\lambda_{sc} = \lambda_{TF} = 1.4a_0 = 7.4 \times 10^{-9}$  cm) is equal to

$$P_{sc}(\pi/2 \leq \theta \leq \pi) = 1.57 \times 10^{-10}, \quad (81)$$

and the value for screening by a metal conduction electron ( $\lambda_{sc} = \lambda_{De,c} = 5 \times 10^{-10}$  cm) is equal to

$$P_{sc}(\pi/2 \leq \theta \leq \pi) = 3.45 \times 10^{-8}. \quad (82)$$

In the case of conduction electron screening in Eq. (82), the screened Coulomb potential energy  $V_{C,sc}(r)$  is defined by the same Eq. (62) with  $\lambda_{TF} \rightarrow \lambda_{sc} = \lambda_{De,c} = 5 \times 10^{-10}$  cm.

For a deuteron projectile with  $E_d = 10$  keV and deuteron target nucleus ( $m_N = m_d$ ), the probability  $P_{sc}(\pi/2 \leq \theta \leq \pi)$  for screening by a deuteron shell electron ( $\lambda_{sc} = \lambda_{TF} = 1.4a_0 = 7.4 \times 10^{-9}$  cm) is equal to

$$P_{sc}(\pi/2 \leq \theta \leq \pi) = 4.73 \times 10^{-8} \quad (83)$$

and for screening by a metal conduction electron ( $\lambda_{sc} = \lambda_{De,c} = 5 \times 10^{-10}$  cm) is equal to

$$P_{sc}(\pi/2 \leq \theta \leq \pi) = 1.04 \times 10^{-5}. \quad (84)$$

Generally, the deep electron screening of the Coulomb barrier (with  $\lambda_{De,c} \ll \lambda_{TF}$ ) could significantly reduce the small-angle elastic scattering dominance, increasing the probabilities of large-angle scattering [thus increasing the astrophysical factor  $S(E)$ ] and successful nuclear fusion events.

For an  $\alpha$  projectile with  $E_\alpha = 3$  MeV and deuteron target nucleus ( $m_N = m_d$ ), the numerical value for  $\sigma_{\alpha-D}$  (total scattering cross section) is

$$\begin{aligned}\sigma_{\alpha-D} &= \int \frac{d\sigma}{d\Omega} \Big|_{\alpha-D} d\Omega \approx \frac{\pi D_{\alpha-D}^2}{\theta_{\min,\alpha}^2} \\ &= \frac{8\pi m_\alpha e^4 \lambda_{TF}^2}{\hbar^2 E_\alpha} = 91.48 \text{ Mb,}\end{aligned}\quad (85)$$

whereas for  $\alpha$  projectile with  $E_\alpha = 1$  MeV and deuteron target nucleus ( $m_N = m_d$ ), the numerical value of  $\sigma_{\alpha-D}$  increases due to the inverse dependence on energy:

$$\sigma_{\alpha-D} = 274.5 \text{ Mb.} \quad (86)$$

The target nucleus recoil energy can be found from the conservation of the total momentum in the elastic projectile

particle-target nucleus scattering process:

$$\vec{p}_N = \vec{p}_p - \vec{p}'_p, \quad (87)$$

where  $\vec{p}_N$  is the target nucleus recoil momentum,  $\vec{p}_p$  is the momentum of the incident projectile particle, and  $\vec{p}'_p$  is the momentum of the scattered projectile particle. Since in elastic scattering  $p_p = |\vec{p}_p| \approx |\vec{p}'_p|$  (for the reason that small-angle scattering is the most probable event), it follows from Eq. (87) that

$$p_N^2 = \vec{p}_N^2 = \vec{p}_p^2 + \vec{p}'_p^2 - 2p_p p'_p \cos\theta \approx 2p_p^2(1 - \cos\theta), \quad (88)$$

where  $\theta$  is the scattering angle. Correspondingly, the target nucleus recoil energy  $E_N(\theta)$  follows from Eq. (88):

$$E_N(\theta) = \frac{p_N^2}{2m_N} \approx \frac{p_p^2}{m_N}(1 - \cos\theta) = \frac{2m_p}{m_N} E_p(1 - \cos\theta), \quad (89)$$

where  $E_p = p_p^2/2m_p$  is the kinetic energy of the projectile particle.

The mean target nucleus recoil energy  $\bar{E}_N$  in single elastic nonrelativistic projectile-target nucleus collision is obtained by averaging of  $E_N(\theta)$  over  $d\Omega$ , and from Eq. (71) with the usual substitution  $\alpha \rightarrow \alpha_p = \theta_{\min,p}^2/2$  it follows that

$$\begin{aligned}\bar{E}_N(\beta_p \ll 1) &= \frac{\hbar^2}{m_N \lambda_{TF}^2} \ln\left(\frac{2}{\theta_{\min,p}}\right) \\ &= \frac{\hbar^2}{m_N \lambda_{TF}^2} \ln\left(\frac{2\lambda_{TF}}{\hbar}\right) \sqrt{2m_p E_p}\end{aligned}\quad (90)$$

since  $\theta_{\min,p} = \hbar/(\lambda_{TF} p_p) = \hbar/(\lambda_{TF} \sqrt{2m_p E_p}) \ll 1$ .

### C. Compton scattering on free deuteron

The differential Klein-Nishina (1929) cross section  $d\sigma_C^{KN}/d\Omega$  per unit solid angle  $d\Omega$  for Compton scattering (of an electron) on a deuteron is given by the standard expression

$$\frac{d\sigma_C^{KN}}{d\Omega} = \frac{r_D^2}{2} \left\{ \frac{1 + \cos^2\theta}{[1 + \varepsilon_D(1 - \cos\theta)]^2} + \frac{\varepsilon_D^2(1 - \cos\theta)^2}{[1 + \varepsilon_D(1 - \cos\theta)]^3} \right\}, \quad (91)$$

where  $r_D$  is the deuteron classical radius  $r_D = e^2/m_D c^2$ ,  $\varepsilon_D = E_\gamma/m_D c^2$  and  $E_\gamma$  is the photon energy.

The total cross section  $\sigma_C^{KN}$  is obtained by integrating the differential cross section for Compton scattering given by Eq. (91) over  $d\Omega$ :

$$\sigma_C^{KN} = \int \frac{d\sigma_C^{KN}}{d\Omega} d\Omega = \int_0^\pi \frac{d\sigma_C^{KN}}{d\Omega} 2\pi \sin\theta d\theta. \quad (92)$$

The above integration produces the standard known formula:

$$\begin{aligned}\sigma_C^{KN} &= 2\pi r_D^2 \left[ \frac{1 + \varepsilon_D}{\varepsilon_D^2} \left( \frac{2(1 + \varepsilon_D)}{1 + 2\varepsilon_D} - \frac{\ln(1 + 2\varepsilon_D)}{\varepsilon_D} \right) \right. \\ &\quad \left. + \frac{\ln(1 + 2\varepsilon_D)}{2\varepsilon_D} - \frac{1 + 3\varepsilon_D}{(1 + 2\varepsilon_D)^2} \right].\end{aligned}\quad (93)$$

For  $E_\gamma = 2$  MeV and  $m_N = m_d$ , the numerical value for  $\sigma_C^{KN}$  is as follows:

$$\sigma_C^{KN} = 49.43 \text{ nb} \quad (94)$$

TABLE II. Mean deuteron recoil energies for various reactions.

Reaction (particle, D)		Total cross section, $\sigma$ (barn)	Mean deuteron recoil energy
Light particles ( $e^-$ , $e^+$ )	$E_e = 2$ MeV	38.41 kb	24.75 meV
Heavy particles	$E_p = 3$ MeV	5.76 Mb	41.4 meV
	$E_d = 3$ MeV	11.51 Mb	42.7 meV
	$E_\alpha = 3$ MeV	91.48 Mb	44 meV
Compton $\gamma$	$E_\gamma = 2$ MeV	49.43 nb	2.13 keV
Neutron, $n$	$E_n = 2.45$ MeV	3 b	1.09 MeV

For small  $\varepsilon_D = E_\gamma/m_D c^2 \ll 1$  the expression for  $\sigma_C^{\text{KN}}$  is reduced to

$$\begin{aligned} \sigma_C^{\text{KN}}(\varepsilon_D \ll 1) &= \frac{8\pi r_D^2}{3} \left( 1 - 2\varepsilon_D + \frac{26}{5}\varepsilon_D^2 - \frac{133}{10}\varepsilon_D^3 + \frac{1144}{35}\varepsilon_D^4 - \dots \right). \end{aligned} \quad (95)$$

For  $E_\gamma = 2$  MeV and  $m_N = m_d$ , the numerical value for  $\sigma_C^{\text{KN}}(\varepsilon_D \ll 1)$ , calculated with the help of Eq. (95), is almost as in Eq. (93), namely

$$\sigma_C^{\text{KN}}(\varepsilon_D \ll 1) = 49.43 \text{ nb}. \quad (96)$$

The deuteron recoil energy  $E_D(\theta)$ , which is the kinetic energy transferred to free (unbounded) deuteron by  $\gamma$  quanta with energy  $E_\gamma$ , is given by the standard known expression:

$$\begin{aligned} E_D(\theta) &= E_\gamma \varepsilon_D \frac{(1 - \cos \theta)}{1 + \varepsilon_D(1 - \cos \theta)}, \\ \varepsilon_D &= \frac{E_\gamma}{m_D c^2}, \end{aligned} \quad (97)$$

where  $\theta$  is the photon scattering angle. When  $E_\gamma \ll m_D c^2$ , (i.e.,  $\varepsilon_D \ll 1$ ) then Eq. (97) is reduced to

$$\begin{aligned} E_D(\theta) &\approx \frac{E_\gamma^2}{m_D c^2} (1 - \cos \theta) = E_\gamma \varepsilon_D (1 - \cos \theta), \\ \varepsilon_D &= \frac{E_\gamma}{m_D c^2} \ll 1. \end{aligned} \quad (98)$$

Mean deuteron recoil energy  $\bar{E}_D$  in single Compton collision is obtained by averaging  $E_D(\theta)$  from Eq. (96) with  $d\sigma_C/d\Omega$  from Eq. (91) over  $d\Omega$ :

$$\bar{E}_D = \frac{\int E_D(\theta) \frac{d\sigma_C^{\text{KN}}}{d\Omega} d\Omega}{\int \frac{d\sigma_C^{\text{KN}}}{d\Omega} d\Omega} = \frac{1}{\sigma_C^{\text{KN}}} \int_0^\pi E_D(\theta) \frac{d\sigma_C^{\text{KN}}}{d\Omega} 2\pi \sin \theta d\theta. \quad (99)$$

The above integration produces the standard known expression

$$\begin{aligned} \bar{E}_D &= E_\gamma [2\varepsilon_D(9 + 51\varepsilon_D + 93\varepsilon_D^2 + 51\varepsilon_D^3 - 10\varepsilon_D^4) \\ &\quad - 3(3 - \varepsilon_D)(1 + \varepsilon_D)(1 + 2\varepsilon_D)^3 \ln(1 + 2\varepsilon_D)] \\ &\quad \times \{6\varepsilon_D(1 + 2\varepsilon_D)[2 + \varepsilon_D(1 + \varepsilon_D)(8 + \varepsilon_D)] \\ &\quad - 3(1 + 2\varepsilon_D)^3 [2 + \varepsilon_D(2 - \varepsilon_D)] \ln(1 + 2\varepsilon_D)\}^{-1}. \end{aligned} \quad (100)$$

When  $\varepsilon_D \ll 1$ , i.e.,  $E_\gamma \ll m_D c^2$ , then Eq. (100) is reduced to

$$\bar{E}_D(\varepsilon_D \ll 1) = E_\gamma \varepsilon_D \left( 1 - \frac{11}{5}\varepsilon_D + \frac{51}{10}\varepsilon_D^2 - \frac{3931}{350}\varepsilon_D^3 + \dots \right). \quad (101)$$

For  $E_\gamma = 2$  MeV and  $m_N = m_d$ , the numerical value for  $\bar{E}_D(\varepsilon_D \ll 1)$  is

$$\bar{E}_D(\varepsilon_D \ll 1) = 2.13 \text{ keV}. \quad (102)$$

In the case of Compton scattering on free electrons, when  $E_\gamma = 2$  MeV, then  $\varepsilon_e = E_\gamma/m_e c^2 = 3.914$ . Then it follows from Eq. (100) that in this case ( $r_D \rightarrow r_e$ ),  $\bar{E}_e = 1.062$  MeV. For  $E_\gamma = 1.022$  MeV,  $\varepsilon_e = E_\gamma/m_e c^2 = 2$ , and it follows from Eq. (100) that  $\bar{E}_e = 0.453$  MeV. Therefore, the kinetic energy transfer to fuel nuclei (D) by energetic photons is much more efficient than by either energetic, light charged particles ( $e^-$ ,  $e^+$ ) or by energetic heavy, charged particles ( $p$ ,  $d$ ,  $\alpha$ ).

Table II provides a comparison of the mean target nucleus recoil energy  $\bar{E}_N$  in single elastic nonrelativistic projectile-target nucleus collision for various projectiles and at different projectile energies. In the table, the target is always a deuteron nucleus ( $m_N = m_d$ ), and the calculation provides a numerical value for  $\bar{E}_D(\beta_p \ll 1)$ .

Thus, we conclude that the kinetic energy transfer to fuel nuclei  $D$  by either energetic light charged particles ( $e^-$ ,  $e^+$ ) or by energetic heavy charged particles ( $p$ ,  $d$ ,  $\alpha$ ) is a very inefficient process unless there is a means to increase the probability of large-angle scattering; for example, via a decreased mean-free path by increased ion and electron densities.

## VI. NEUTRON ELASTIC SCATTERING ON DEUTERON NUCLEI

Since the deuteron nucleus possesses just single (ground) energy level, the neutron scattering on deuteron is elastic scattering process, if energy of neutron is below the disintegration of deuteron by neutron (the deuteron disintegration threshold by neutron  $K_n^{\text{th}} = 3.4$  MeV). In this case, it is well known [21] that the neutron elastic cross section  $\sigma_{\text{sc}}(\theta_{\text{CM}})$  is isotropic in the center of mass (CM) frame; that is,

$$\sigma_{\text{sc}}(\theta_{\text{CM}}) = \frac{\sigma_{\text{sc}}}{4\pi}, \quad (103)$$

where  $\theta_{\text{CM}}$  is the neutron scattered angle in the CM frame, and  $\sigma_{\text{sc}}$  is the total neutron elastic cross section. The scattering

angle  $\theta_{\text{lab}}$  in the lab frame is related to  $\theta_{\text{CM}}$  as

$$\tan \theta_{\text{lab}} = \frac{m_d \sin \theta_{\text{CM}}}{m_n + m_d \cos \theta_{\text{CM}}}, \quad (104)$$

where  $m_n$  and  $m_d$  are the neutron and deuteron mass, respectively.

Since the scattered angles  $\theta_{\text{CM}}$  and  $\theta_{\text{lab}}$  are different, the angular distributions of scattered particles in CM and lab frames are also different. However, the number of scattered particles in the corresponding solid angle  $d\Omega(\theta_{\text{CM}})$  in the CM frame and in solid angle  $d\Omega(\theta_{\text{lab}})$  in the lab frame must be the same:

$$\sigma_{\text{sc}}(\theta_{\text{lab}})d\Omega(\theta_{\text{lab}}) = \sigma_{\text{sc}}(\theta_{\text{CM}})d\Omega(\theta_{\text{CM}}). \quad (105)$$

However,  $d\Omega(\theta_{\text{CM}}) = 2\pi \sin(\theta_{\text{CM}})d\theta_{\text{CM}}$  and  $d\Omega(\theta_{\text{lab}}) = 2\pi \sin(\theta_{\text{lab}})d\theta_{\text{lab}}$ ; therefore, Eq. (92) becomes

$$\sigma_{\text{sc}}(\theta_{\text{lab}}) \sin(\theta_{\text{lab}})d\theta_{\text{lab}} = \sigma_{\text{sc}}(\theta_{\text{CM}}) \sin(\theta_{\text{CM}})d\theta_{\text{CM}}. \quad (106)$$

With the help of Eq. (104) it follows from Eq. (106) that the angular distribution of scattered particles in the lab frame can be determined from the corresponding angular distribution of scattered particles in the CM frame [21], as follows:

$$\sigma_{\text{sc}}(\theta_{\text{lab}}) = \sigma_{\text{sc}}(\theta_{\text{CM}}) \frac{[m_n^2 + m_d^2 + 2m_n m_d \cos(\theta_{\text{CM}})]^{3/2}}{m_d^2 [m_d + m_n \cos(\theta_{\text{CM}})]}. \quad (107)$$

The relation between scattered neutron velocities,  $\vec{v}'_{n,\text{CM}}$  in the CM frame and  $\vec{v}'_{n,\text{lab}}$  in the lab frame, is given by the simple formula

$$\vec{v}'_{n,\text{lab}} = \vec{v}'_{n,\text{CM}} + \vec{V}_{\text{CM}}, \quad V_{\text{CM}} = \frac{m_n}{m_n + m_d} \vec{v}_n, \quad (108)$$

where  $\vec{V}_{\text{CM}}$  is the CM frame velocity, and  $\vec{v}_n$  is the neutron velocity in the lab frame. Correspondingly, the relation between neutron and deuteron velocities  $\vec{v}_{n,\text{CM}}$  and  $\vec{v}_{d,\text{CM}}$  in the CM frame and  $\vec{v}_n$  and  $\vec{v}_d$  in the lab frame are as follows:

$$\begin{aligned} \vec{v}_{n,\text{CM}} &= \vec{v}_n - \vec{V}_{\text{CM}} = \frac{m_d}{m_n + m_d} \vec{v}_n, \\ \vec{v}_{d,\text{CM}} &= -\vec{V}_{\text{CM}} = -\frac{m_n}{m_n + m_d} \vec{v}_n, \quad \text{and} \quad \vec{v}_d = 0. \end{aligned} \quad (109)$$

Since the magnitude of neutron velocity in CM does not change after collision, i.e.,  $v'_{n,\text{CM}} = v_{n,\text{CM}}$ , it follows with the help of Eqs. (108) and (109) that

$$\begin{aligned} v_{n,\text{lab}}^2 &= v_{n,\text{CM}}^2 + V_{\text{CM}}^2 + 2v_{n,\text{CM}}V_{\text{CM}} \cos \theta_{\text{CM}} \\ &= \frac{(m_n^2 + m_d^2 + 2m_n m_d \cos \theta_{\text{CM}})}{(m_n + m_d)^2} v_n^2. \end{aligned} \quad (110)$$

Rewriting Eq. (110) in terms of the neutron kinetic energy  $K'_n$  after and the neutron kinetic energy  $K_n$  before yields

$$K'_n = \frac{(m_n^2 + m_d^2 + 2m_n m_d \cos \theta_{\text{CM}})}{(m_n + m_d)^2} K_n. \quad (111)$$

It is convenient to introduce the new parameter  $\alpha_n$  by the following definition [21]:

$$\alpha_n = \frac{(m_d - m_n)^2}{(m_d + m_n)^2}. \quad (112)$$

Then, in term of the new parameter  $\alpha_n$ , Eq. (111) is reduced to

$$K'_n = \frac{1}{2} K_n [(1 + \alpha_n) + (1 - \alpha_n) \cos \theta_{\text{CM}}]. \quad (113)$$

From Eq. (113) it is easy to find out that the kinetic energy  $K'_n$  is in the following limits ( $0 \leq \theta_{\text{CM}} \leq \pi$ ):

$$\alpha_n K_n \leq K'_n \leq K_n. \quad (114)$$

The probability distribution  $P(K_n \rightarrow K'_n)dK'_n$  is, by definition, the probability that the neutron with initial kinetic energy  $K_n$  will acquire kinetic energy in the energy gap ( $K'_n, K'_n + dK'_n$ ) after the collision. The probability that the neutron will be scattered in interval  $(\theta_{\text{CM}}, \theta_{\text{CM}} + d\theta_{\text{CM}})$  is given by

$$\frac{\sigma_{\text{sc}}(\theta_{\text{CM}})d\Omega(\theta_{\text{CM}})}{\sigma_{\text{sc}}} = \frac{\sigma_{\text{sc}}(\theta_{\text{CM}})2\pi \sin(\theta_{\text{CM}})d\theta_{\text{CM}}}{\sigma_{\text{sc}}}, \quad (115)$$

where  $\sigma_{\text{sc}}(\theta_{\text{CM}})$  is the neutron differential elastic cross section and  $\sigma_{\text{sc}}$  is the total neutron elastic cross section in CM. It is clear that they are the same probabilities:

$$P(K_n \rightarrow K'_n)dK'_n = -\frac{\sigma_{\text{sc}}(\theta_{\text{CM}})2\pi \sin(\theta_{\text{CM}})}{\sigma_{\text{sc}}} d\theta_{\text{CM}} \quad (116)$$

since  $d\theta_{\text{CM}} > 0 \rightarrow dK'_n < 0$ , thus providing the positivity of the probability  $P(K_n \rightarrow K'_n) > 0$ .

From Eq. (113) it follows that

$$dK'_n = -\frac{1}{2} K_n (1 - \alpha_n) \sin \theta_{\text{CM}} d\theta_{\text{CM}}. \quad (117)$$

Substitution of Eq. (117) into Eq. (116) yields [21]

$$\begin{aligned} P(K_n \rightarrow K'_n) &= \frac{4\pi \sigma_{\text{sc}}(\theta_{\text{CM}})}{K_n (1 - \alpha_n) \sigma_{\text{sc}}} \\ &\text{for} \\ &(\alpha_n K_n \leq K'_n \leq K_n). \end{aligned} \quad (118)$$

Since the neutron elastic cross section  $\sigma_{\text{sc}}(\theta_{\text{CM}})$  is isotropic in the CM frame, then substitution of  $\sigma_{\text{sc}}(\theta_{\text{CM}}) = \sigma_{\text{sc}}/4\pi$  from Eq. (103) into Eq. (118) yields

$$\begin{aligned} P(K_n \rightarrow K'_n) &= \frac{1}{K_n (1 - \alpha_n)} \\ &\text{for} \\ &(\alpha_n K_n \leq K'_n \leq K_n). \end{aligned} \quad (119)$$

Therefore, the kinetic energy probability distribution  $P(K_n \rightarrow K'_n)$  is independent of  $K'$  in the whole interval ( $\alpha_n K_n \leq K'_n \leq K_n$ ) [21].

## VII. NEUTRON ENERGY LOSS IN ELASTIC COLLISIONS WITH DEUTERON NUCLEI

By definition, the average neutron kinetic energy  $\bar{K}'_n$  after elastic collision is obtained by averaging  $\bar{K}'_n$  with the probability distribution  $P(K_n \rightarrow K'_n)$  given by Eq. (119):

$$\bar{K}'_n = \frac{\int_{\alpha_n K_n}^{K_n} K'_n P(K_n \rightarrow K'_n) dK'_n}{\int_{\alpha_n K_n}^{K_n} P(K_n \rightarrow K'_n) dK'_n} = \frac{1}{2} (1 + \alpha_n) K_n. \quad (120)$$

The average kinetic energy transferred from neutron to deuteron nucleus in elastic collision is equal to  $K_n - \bar{K}'_n$  [see

also Eq. (112)]:

$$\begin{aligned}\bar{K}'_d &= K_n - \bar{K}'_n = \frac{1}{2}(1 - \alpha_n)K_n \\ &= \frac{2m_n m_d}{(m_n + m_d)^2} K_n = \frac{4}{9} K_n,\end{aligned}\quad (121)$$

which is equal to one-half of the maximum energy transfer in a head-on collision [21]:

$$K'_{d,\max} = \frac{4m_n m_d}{(m_n + m_d)^2} K_n. \quad (122)$$

For a neutron projectile on deuteron target nucleus, with the total elastic cross section of the order of

$$\sigma_{\text{sc}} \sim 3 \text{ bn} (25 \text{ meV} \leq K_n \leq 2 \text{ MeV}). \quad (123)$$

Consequently, the kinetic energy transfer to fuel nuclei (D) by energetic neutrons is the most efficient process compared to energy transferred by energetic light charged particles ( $e^-$ ,  $e^+$ ), by energetic heavy charged particles ( $p$ ,  $d$ ,  $\alpha$ ), or even by energetic photons.

### VIII. SUMMARY

This study indicates the crucial role of electron screening on the overall efficiency of nuclear fusion events between charged particles. We show that neutrons are far more efficient than energetic charged particles, such as light particles ( $e^-$ ,  $e^+$ ) or heavy particles ( $p$ ,  $d$ ,  $\alpha$ ) in transferring kinetic energy to fuel nuclei (D) to initiate fusion processes. We provide a theoretical framework for  $d$ -D nuclear fusion reactions in high-density cold fuel nuclei embedded in metal lattices, with a small fraction of fuel activated by hot neutrons, which in this study are produced by  $\gamma$  induced photodissociation. We also establish the important role of electron screening in increasing

the relative probability  $P_{\text{sc}}(\pi/2 \leq \theta \leq \pi)$  to scatter in the back hemisphere ( $\pi/2 \leq \theta \leq \pi$ ), an essential requirement for subsequent tunneling of reacting nuclei to occur. This will correspondingly be reflected as an increase in the astrophysical factor  $S(E)$ . We also clarify the applicability of the concept of electron screening potential energy  $U_e$  to the calculation of the nuclear cross section enhancement factor  $f(E)$ . We demonstrate that the screened Coulomb potential of the target ion is determined by the nonlinear Vlasov potential and not by the Debye potential. In general, the effect of screening becomes important at low kinetic energy of the projectile. We examine the range of applicability of both the analytical and asymptotic expressions for the well-known electron screening lattice potential energy  $U_e$ , which is valid only for  $E \gg U_e$  ( $E$  is the energy in the center of mass reference frame). We demonstrate that for  $E \leq U_e$ , a direct calculation of Gamow factor for screened Coulomb potential is required to avoid unreasonably high values of the enhancement factor  $f(E)$  by the analytical—and more so by the asymptotic—formulas.

### ACKNOWLEDGMENTS

The authors gratefully acknowledge the assistance of many people that supported this effort, including condensed matter physics guidance and technical consultation from Dr. L. DeChiaro (U.S. Navy). We gratefully acknowledge technical input and stimulating discussions from Dr. M. Forsbacka (NASA HQ), Dr. C. Iannello (NASA KSC), Dr. R. Litchford (NASA MSFC), and Dr. J. Scott (NASA JSC), as well as L. Dudzinski (Planetary Sciences Division, NASA HQ). We are also grateful for Dr. J. Gilland and Dr. T. Gray for valuable comments on the manuscript. Funding for this work was provided by NASA Headquarters Planetary Sciences Division, Science Mission Directorate.

- 
- [1] B. M. Steinetz *et al.*, *Phys. Rev. C* **101**, 044610 (2020).  
 [2] B. R. Martin, *Nuclear and Particle Physics* (John Wiley, West Sussex, 2009), p. 264.  
 [3] C. Rolfs and W. Rodney, *Cauldrons in Cosmos* (University of Chicago Press, Chicago, London, 1988).  
 [4] F. Strieder, C. Rolfs, C. Spitaleri, and P. Corvisiero, *Naturwissenschaften* **88**, 461 (2001).  
 [5] C. Bonomo *et al.*, *Nucl. Phys. A* **719**, C37 (2003).  
 [6] U. Greife, F. Gorris, M. Junker, C. Rolfs, and D. Zahnow, *Z. Phys. A* **351**, 107 (1995).  
 [7] F. Raiola *et al.*, *Eur. Phys. J. A* **13**, 377 (2002).  
 [8] F. Raiola *et al.*, *Phys. Lett. B* **547**, 193 (2002).  
 [9] K. Czerski, A. Heide, and G. Ruprecht, *Eur. Phys. J. A* **27**, 83 (2006).  
 [10] E. E. Salpeter, *Austr. J. Phys.* **7**, 373 (1954).  
 [11] H. J. Assenbaum, K. Langanke, and C. Rolfs, *Z. Phys. A* **327**, 461 (1987).  
 [12] Y. Fukai, *The Metal-Hydrogen System* (Springer-Verlag, New York, 2005).  
 [13] L. D. Landau and E. M. Lifshitz, *Statistical Physics*, 3rd ed., Part 1 (Pergamon, Oxford, New York, 1980).  
 [14] J. D. Jackson, *Classical Electrodynamics*, 3rd ed. (John Wiley, New York, 1999).  
 [15] P. K. Shukla, *Phys. Plasmas* **8**, 1791 (2001).  
 [16] V. Pines, M. Zlatkowski, and A. Chait, *Adv. Space Res.* **46**, 942 (2010).  
 [17] C. Kittel, *Introduction to Solid State Physics*, 8th ed. (John Wiley, New York, 2004).  
 [18] J. Kasagi, in *Proceedings of the 14th International Conference on Condensed Matter Nuclear Science (ICCF-14)* (International Society for Condensed Matter Science, Washington, DC, 2008), Vol. 1, p. 318.  
 [19] P. Sigmund, *Particle Penetration and Radiation Effects* (Springer, New York, 2007).  
 [20] M. Dapor, *Electron-Beam Interactions with Solids* (Springer, New York, 2003).  
 [21] J. R. Lamarsh, *Introduction to Nuclear Reactor Theory* (American Nuclear Society, Inc., La Grange Park, 2002).